Mon. Not. R. Astron. Soc. **000**, 1–?? (2005) Printed 5th February 2008 (MN LaTeX style file v2.2)

arXiv:astro-ph/0507560v1 23 Jul 2005

Cooling of Akmal-Pandharipande-Ravenhall neutron star models

M. E. Gusakov,[1⋆] A. D. Kaminker,[1] D. G. Yakovlev,[1] and O. Y. Gnedin[2]
[1] *Ioffe Physical Technical Institute, Politekhnicheskaya 26, 194021 Saint-Petersburg, Russia,*
e-mail: gusakov@astro.ioffe.ru, kam@astro.ioffe.ru, yak@astro.ioffe.ru
[2] *Ohio State University, 760 1/2 Park Street, Columbus, OH 43215, USA,*
e-mail: ognedin@astronomy.ohio-state.edu

Released 2005 Xxxxx XX

ABSTRACT

We study the cooling of superfluid neutron stars whose cores consist of nucleon matter with the Akmal-Pandharipande-Ravenhall equation of state. This equation of state opens the powerful direct Urca process of neutrino emission in the interior of most massive neutron stars. Extending our previous studies (Gusakov et al. 2004a, Kaminker et al. 2005), we employ phenomenological density-dependent critical temperatures $T_{\rm cp}(\rho)$ of strong singlet-state proton pairing (with the maximum $T_{\rm cp}^{\rm max} \sim 7 \times 10^9$ K in the outer stellar core) and $T_{\rm cnt}(\rho)$ of moderate triplet-state neutron pairing (with the maximum $T_{\rm cnt}^{\rm max} \sim 6 \times 10^8$ K in the inner core). Choosing properly the position of $T_{\rm cnt}^{\rm max}$ we can obtain a representative class of massive neutron stars whose cooling is intermediate between the cooling enhanced by the neutrino emission due to Cooper pairing of neutrons in the absence of the direct Urca process and the very fast cooling provided by the direct Urca process non-suppressed by superfluidity.

Key words: Stars: neutron – dense matter

1 INTRODUCTION

Fundamental properties of supranuclear matter in the cores of neutron stars, such as the equation of state and critical temperatures of baryon superfluidity, are still poorly known. In particular, they can be studied (e.g., Yakovlev & Pethick 2004 and references therein) by comparing the theory of cooling isolated neutron stars with observations of thermal radiation (e.g., Pavlov et al. 2002, Pavlov & Zavlin 2003) from these stars.

In this paper we study the cooling of superfluid neutron stars with the cores composed of neutrons, protons, electrons, and muons. We employ model equations of state (EOSs) of neutron star cores based on the EOS of Akmal, Pandharipande & Ravenhall (1998) (APR, Section 4) which is currently assumed to be the most elaborated EOS. It opens the powerful direct Urca process of neutrino emission (Lattimer et al. 1991) in neutron stars with masses slightly lower than the maximum mass. Our cooling models will be based on standard (nucleon) composition of neutron stars and standard neutrino processes (no "exotic" physics involved).

The paper extends our previous studies (Gusakov et al. 2004a and Kaminker et al. 2005; hereafter Paper I and Paper II, respectively) of cooling neutron stars with superfluid nucleon cores, where the direct Urca process is forbidden. In this scenario, observations of cold neutron stars (e.g., of the Vela pulsar) are explained by the enhanced neutrino emission due to Cooper pairing of neutrons in neutron star cores. Page et al. (2004), who suggested a similar cooling scenario, called it "Minimal Cooling". Note, however, that the realization of this scheme by Page et al. and in Papers I and II is different (see Paper II for details).

In Papers I and II we employed the EOS of Douchin & Haensel (2001) (the DH EOS, which forbids the direct Urca process in all stars) and a model of triplet-state neutron pairing with the maximum of the critical temperature $T_{\rm cnt}^{\rm max} \approx 6 \times 10^8$ K in the inner stellar core. This pairing is needed to produce an enhanced neutrino cooling of massive stars and explain the observations of neutron stars coldest for their age (such as the Vela pulsar). In Paper I we assumed also strong singlet-state proton pairing in the outer stellar core, with $T_{\rm cp}^{\rm max} \gtrsim 5 \times 10^9$ K. It slows down the cooling of low-mass neutron stars and enables us to interpret the observations of stars warmest for their age (e.g., RX J0822–4300 or PSR B1055–52). In Paper II we included the effects of surface (accreted) envelopes of light elements. They allowed us to explain the observations of warmest stars assuming weaker proton pairing ($T_{\rm cp}^{\rm max} \gtrsim 10^9$ K).

Now we will add the effect of the direct Urca process in

⋆ Send offprint request to: M. E. Gusakov most massive stars in accordance with the APR EOS. We will use similar (but slightly different) models for strong proton pairing and moderate neutron pairing in the stellar core. These superfluid models are sufficient to explain current observations of all cooling neutron stars without opening the direct Urca process. However, most massive stars predicted by the APR EOS can be much colder than the stars observed today and, we will focus on their properties. For simplicity, we will neglect the effects of accreted envelopes. They are unimportant for massive neutron stars; we could easily include them as in Paper II.

2 OBSERVATIONS

Table 1 summarizes the observations of isolated (cooling) middle-aged neutron stars (10^3 yr $\lesssim t \lesssim 10^6$ yr), whose thermal surface radiation has been detected or constrained. We present the estimated stellar ages t and the effective surface temperatures T_s^∞ (redshifted for a distant observer). The data are described in Paper I and slightly corrected in Paper II.

The surface temperatures of some sources (labeled by $^{a)}$) have been obtained by fitting their thermal radiation spectra with hydrogen atmosphere models. Such models are more consistent with other information on these sources (e.g., Pavlov & Zavlin 2003) than the blackbody model. For other sources (e.g., for Geminga and PSR B1055–52, labeled by $^{b)}$) we present the values of T_s^∞ inferred using the blackbody spectrum because this spectrum is more consistent for these sources. The surface temperature of RX J1856.4–3754 is still uncertain. Following Paper I we adopt the upper limit $T_s^\infty < 0.65$ MK. Finally, T_s^∞ for RX J0720.4–3125 is taken from Motch et al. (2003), who interpreted the observed spectrum with a model of a hydrogen atmosphere of finite depth.

Note also new results by Kargaltsev et al. (2005) for Geminga presented in Table 1. As in Papers I and II we retain 20% errorbars for this source.

3 COOLING WITHOUT THE DIRECT URCA PROCESS

We will simulate neutron star cooling using our general relativistic cooling code (Gnedin et al. 2001) which calculates cooling curves (the dependence of T_s^∞ on the stellar age t). At the initial cooling stage ($t \lesssim 100$ yr) a star cools via neutrino emission but the stellar interior is non-isothermal. At the next stage (10^2 yr $\lesssim t \lesssim 10^5$ yr) the neutrino emission dominates but the interior is isothermal. Later ($t \gtrsim 10^5$ yr) the star cools mainly via the surface photon emission.

For the adopted EOSs, all constituents of dense matter (nucleons, electrons, and muons) exist everywhere in the stellar core, except for muons which appear at $\rho \sim 2.0 \times 10^{14}$ g cm^{-3}. As in Paper I we use the relation between the effective surface temperature and the temperature at the bottom of the heat-blanketing iron envelope calculated by Potekhin et al. (2003).

Neutron star cooling is strongly affected by superfluidity of nucleons in stellar interiors. Any superfluidity is characterized by a density-dependent profile of critical temperature $T_c(\rho)$. In principle, an EOS and a superfluidity model, employed in cooling simulations, have to be obtained from the same nuclear Hamiltonian. However, such calculations are currently absent and one usually treats the EOS and superfluid properties as independent. Although this approach is simplified it sounds reasonable at the present stage of the investigation because the EOS is the bulk property of the matter (determined by the entire Fermi see of baryons) while superfluidity is a Fermi-surface phenomenon and can be, therefore, relatively independent. Microscopic theories predict two main types of superfluidity inside the neutron star core: singlet-state proton pairing ($T_c = T_{cp}$) and triplet-state neutron pairing ($T_c = T_{cnt}$). These theories give a large scatter of critical temperatures depending on a nucleon-nucleon interaction model and a many-body theory employed (e.g., Lombardo & Schulze 2001, Yakovlev et al. 1999; see also recent papers by Schwenk & Friman 2004, Takatsuka & Tamagaki 2004, Zuo et al. 2004, Tanigawa et al. 2004). As in Papers I and II, we will treat $T_{cp}(\rho)$ and $T_{cnt}(\rho)$ as phenomenological functions of ρ which do not contradict some microscopic calculations. These functions could be (in principle) constrained by comparing theoretical cooling curves with observations.

Superfluidity of nucleons affects the nucleon heat capacity and suppresses neutrino processes involving superfluid nucleons: Urca and nucleon-nucleon bremsstrahlung processes (as reviewed, e.g., by Yakovlev et al. 1999). Moreover, superfluidity induces an additional neutrino emission mechanism associated with Cooper pairing of nucleons (Flowers, Ruderman & Sutherland 1976). All these effects of superfluidity are included into our cooling code in the same manner as in Papers I and II.

In Fig. 1 we plot two models of nucleon pairing employed in the present paper, model p for strong singlet-state proton pairing (with the peak of $T_{cp}(\rho)$ approximately equal to $T_{cp}^{max} \approx 6.8 \times 10^9$ K); and model nt for moderate triplet-state neutron pairing ($T_{cnt}^{max} \sim 6 \times 10^8$ K). Models p and nt slightly differ from similar models p1 and nt1 in Papers I and II. Note that the curves $T_{cp}(\rho)$ and $T_{cnt}(\rho)$ are almost insensitive to the employed EOS: DH (Papers I and II) and APR I, II, and III (Section 4). Our pairing model nt seems specific (shifted to too high densities ρ at which neutron pairing dies out according to many microscopic calculations). However similar models have been obtained from some microscopic theories (e.g., see the curve $m^* = 0.73$ in Fig. 1 of Takatsuka & Tamagaki 1997).

Figure 2 illustrates the cooling scenario of Paper I (to be compared with new scenarios). We plot a family of cooling curves calculated for the DH EOS, which forbids the direct Urca process in all stable neutron stars ($M \leqslant M_{max} = 2.05 M_\odot$). The curves refer to neutron stars with (gravitational) masses M from 1.00 to 2.04 $M_\odot$ (from top to bottom).

The curves explain all the data from Table 1. The coldest objects can be interpreted as most massive neutron stars with moderate neutron pairing in the inner cores (at densities $\rho \gtrsim 8 \times 10^{14}$ g cm^{-3}). When the internal temperature of a massive star falls below T_{cnt}^{max}, the cooling is noticeably enhanced by the neutrino emission due to Cooper pairing of neutrons. This enhancement is sufficient to explain the observations of neutron stars coldest for their age, particularly, PSR J0205+6449, RX J0007.0+7303, the Vela and Geminga pulsars. Note that the data on RX J0007.0+7303

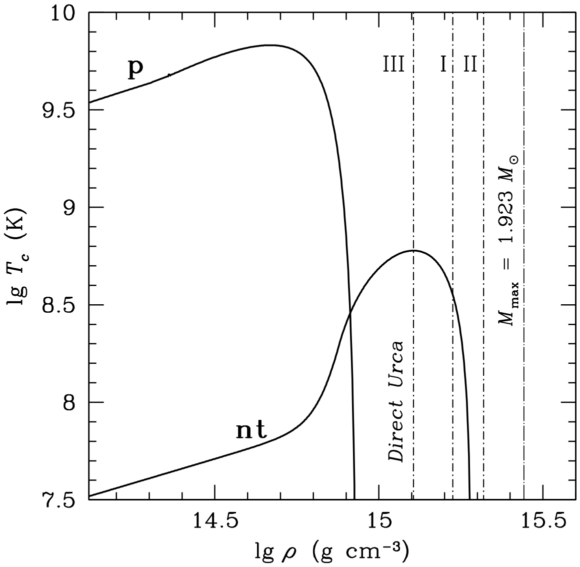

Figure 1. Density dependence of the critical temperatures for model p of singlet-state proton pairing and model nt of triplet-state neutron pairing in a neutron star core. Three vertical dot-and-short-dashed lines indicate the thresholds of the direct Urca process for the EOSs APR I, II, and III discussed in Section 4. The vertical dot-and-long-dashed line shows the central density of a maximum-mass neutrons star for APR I; two other maximum-mass lines are almost the same.

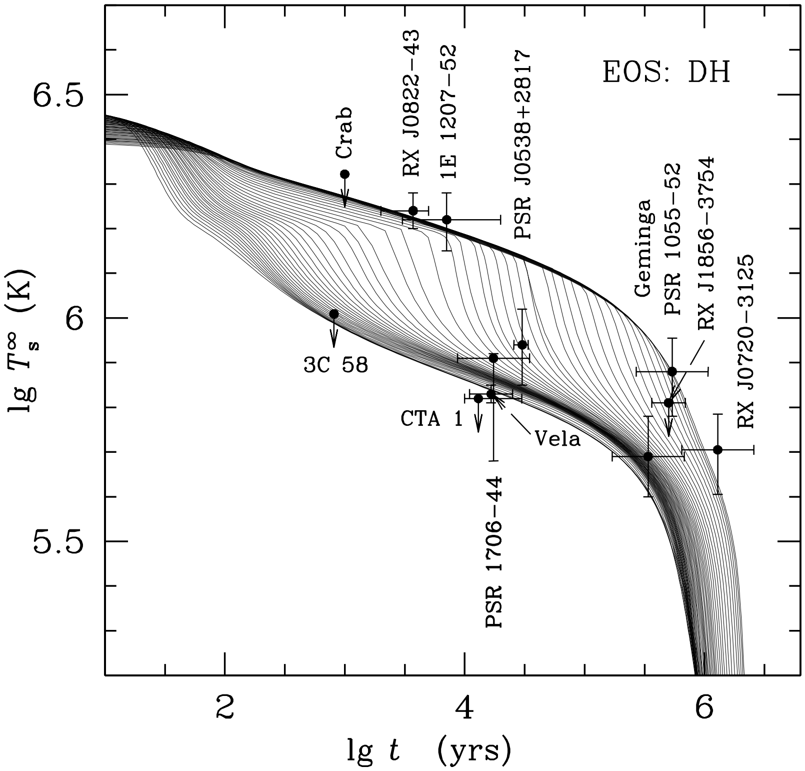

Figure 2. Observational limits on surface temperatures of twelve isolated neutron stars (Table 1) compared with theoretical cooling curves calculated for the DH EOS (no direct Urca process) and for models p and nt of nucleon pairing (Fig. 1). Fifty three curves refer to neutron stars of masses from 1.00 to 2.04 $M_\odot$ (from top to bottom, with the step 0.02 $M_\odot$).

Table 1. Observational limits on surface temperatures of isolated neutron stars

Source	t [kyr]	$T_{\rm s}^{\infty}$ [MK]	Confid. of $T_{\rm s}^{\infty}$	References
PSR J0205+6449 (in 3C 58)	0.82	<1.02 $^{b)}$	99.8%	Slane et al. (2004)
Crab	1	<2.0 $^{b)}$	99.8%	Weisskopf et al. (2004)
RX J0822–4300	2–5	1.6–1.9 $^{a)}$	90%	Zavlin et al. (1999)
1E 1207.4–5209	3–20	1.4–1.9 $^{a)}$	90%	Zavlin et al. (2004)
RX J0007.0+7303 (in CTA 1)	10–30	<0.66 $^{b)}$	–	Halpern et al. (2004)
Vela	11–25	0.65–0.71 $^{a)}$	68%	Pavlov et al. (2002)
PSR B1706–44	$\sim$17	$0.82^{+0.01}_{-0.34}$ $^{a)}$	68%	McGowan et al. (2004)
PSR J0538+2817	30 ± 4	~ 0.87 $^{a)}$	–	Zavlin & Pavlov (2004)
Geminga	$\sim$340	~ 0.5 $^{b)}$	–	Kargaltsev et al. (2005)
RX J1856.4–3754	$\sim$500	<0.65	–	see Paper I
PSR B1055–52	$\sim$540	$\sim$0.75 $^{b)}$	–	Pavlov & Zavlin (2003)
RX J0720.4–3125	$\sim$ 1300	~ 0.51 $^{a)}$	–	Motch et al. (2003)

$^{a)}$ Inferred using a hydrogen atmosphere model
$^{b)}$ Inferred using the black-body spectrum

are explained in this way only marginally. However, taking into account that real uncertainties of $T_{\rm s}^{\infty}$ and t can be larger than the adopted ones we can accept this explanation as successful. All stars with the central density higher than the density at which neutron pairing dies out ($\rho_{\rm c} \gtrsim 2 \times 10^{15}$ g cm^{-3} in Fig. 1) cool nearly as fast as the star with $M = M_{\rm max}$. This gives the lower dense bunch of cooling curves of massive neutron stars (with $\rho_c \gtrsim 2 \times 10^{15}$ g cm^{-}3) in Fig. 2.

There is the other (upper) dense bunch of cooling curves of low-mass stars ($M \lesssim 1.1\, M_\odot$). The central densities of such stars are $\rho_{\rm c} \lesssim 8 \times 10^{14}$ g cm^{-3}. Proton pairing is strong ($T_{\rm cp}(\rho) \gtrsim 3 \times 10^9$ K) everywhere in their cores (Fig 1). It completely suppresses all neutrino processes involving protons and substantially slows down the cooling.

Finally, there is a class of medium-mass neutron stars which show intermediate cooling. Their cooling curves fill in the space between the upper dense bunch of cooling curves (low-mass stars) and the lower dense bunch (high-mass stars). We can treat PSR B1706–44, PSR J0538+2817, and RX J1856.4–3754 as medium-mass stars.

Although this scenario is consistent with all current observations, colder stars could be detected in the future. An indirect evidence for the existence of such stars is given by a non-detection of compact central objects in four supernova remnants (Kaplan et al. 2004). If neutron stars are present there, they should be really cold. It would be impossible to explain them with the cooling scenario presented in Fig. 2, but they could be interpreted adopting the APR EOS.

4 COOLING OF APR NEUTRON STARS

4.1 Equations of state

Let us employ three EOSs of dense matter, APR I, APR II, and APR III. They represent a useful parameterization of the well-known EOS obtained by Akmal et al. (1998) (model Argon V18 + δv + UIX*). This parameterization was proposed by Heiselberg & Hjorth-Jensen (1999). We use the same parameters for the compressional modulus of the nucleon matter and vary only the parameter γ in the expression for symmetry energy, $S(n_{\rm b}) = S_0\,(n_{\rm b}/n_0)^\gamma$, where $S_0 = 32$ MeV; $n_{\rm b}$ is the baryon number density, and $n_0 = 0.16$ fm^{-3} is the baryon number density in saturated nuclear matter. Specifically, we have taken γ=0.6, 0.575, and 0.643 for the APR EOSs I, II, and III, respectively. These EOSs differ mainly in the threshold densities for opening the direct Urca process (see Fig. 1).

Some properties of the EOSs and associated neutron star models are illustrated in Figs. 1 and 3 and in Table 2. For comparison, in Fig. 3 and Table 2 we include also the data on the DH EOS (Douchin & Haensel 2001) and the original APR EOS (Akmal et al. 1998). The APR EOS corresponds to the nucleon matter with the appearance of neutral pion condensation. To plot this EOS in Fig. 3 we use the parameterization proposed by Haensel & Potekhin (2004), with the values of fit parameters provided by A.Y. Potekhin (2004, private communication).

Table 2 gives masses M, central densities $\rho_{\rm c}$, and circumferential radii R of two stellar configurations. The first configuration is the most massive stable neutron star. The values of $M_{\rm max}$ indicate that all five EOSs are moderately stiff and similar. The second configuration refers to the onset of the direct Urca process, ($\rho_{\rm c} = \rho_{\rm D}$, $M = M_{\rm D}$); it is absent for the DH EOS. The APR III EOS implies larger symmetry energy at supranuclear densities (larger γ) and larger proton fraction than the EOSs APR I and II. Accordingly, the direct Urca process opens at lower density for APR III.

Figure 3 shows the pressure-density (left) and the mass-central density (right) diagrams for all five EOSs. According to the left panel, all EOSs are similar. The $P(\rho)$ curves intersect in one point, $\rho \simeq 8.5 \times 10^{14}$ g cm^{-3}. However, small differences in the EOSs lead to noticeable differences in neutron star configurations, particularly, in the mass-density relations $M(\rho_{\rm c})$ (the right panel). Corresponding proton fractions and direct Urca thresholds are also different (Table 2 and Fig. 1).

4.2 Beyond the direct Urca threshold

In contrast to the cooling scenarios in Papers I and II we use the EOS which opens the direct Urca process in massive

Table 2. Neutron star models for the EOSs DH, APR I, II, III, and APR

Model	Main parameters	DH	APR	APR I $\gamma = 0.6$	APR II 0.575	APR III 0.643
Maximum	$M_{\max}/M_\odot$	2.05	2.20	1.923	1.919	1.929
mass	$\rho_{\max}/10^{15}$ g cm^{-3}	2.86	2.74	2.759	2.774	2.731
model	R km	9.99	9.99	10.32	10.28	10.39
Direct Urca	$M_{\rm D}/M_\odot$	–	2.01	1.829	1.891	1.685
threshold	$\rho_{\rm D}/10^{15}$ g cm^{-3}	–	1.56	1.680	2.084	1.275
model	R km	–	10.95	11.27	10.83	11.83

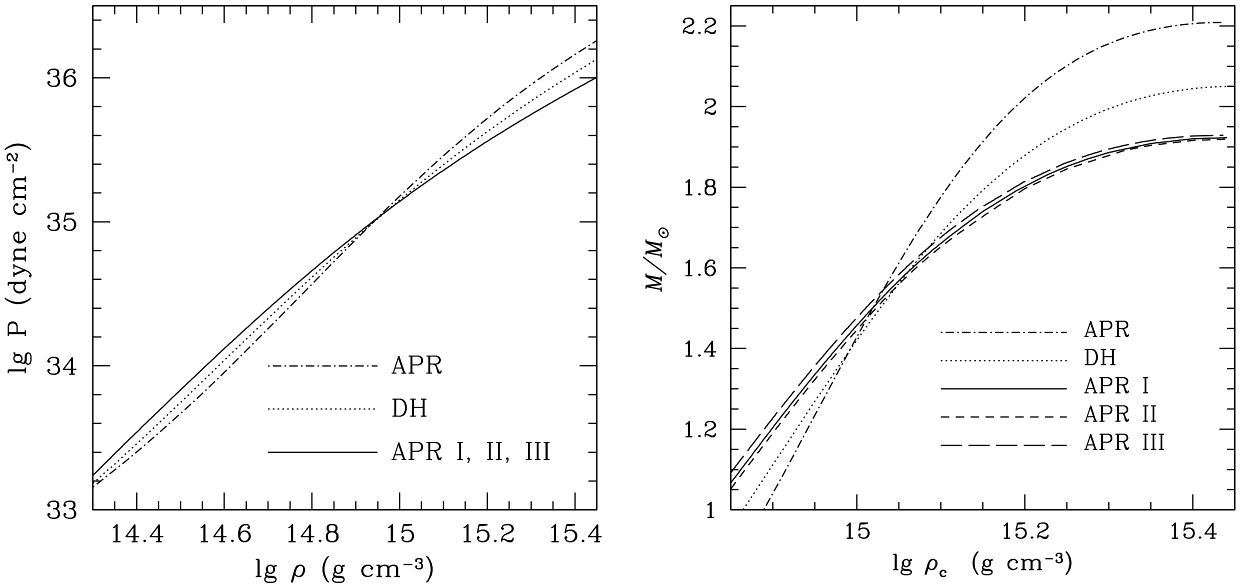

Figure 3. Pressure – density (left) and mass – central density (right) diagrams for five EOSs. The APR EOS was suggested by Akmal et al. (1998). The EOSs APR I, II, and III refer to different values of γ (see Table 2) in the parameterization proposed by Heiselberg & Hjorth-Jensen (1999). The DH EOS was derived by Douchin & Haensel (2001).

neutron stars. Moreover, contrary to our older cooling scenarios (e.g., Kaminker et al. 2002, Yakovlev & Pethick 2004 and references therein) the direct Urca process is now open at densities at which proton superfluidity dies out (Fig. 1), in agreement with some recent calculations of proton pairing in dense matter (e.g., Takatsuka & Tamagaki 1997, 2004, Zuo et al. 2004).

Figure 4 shows a family of cooling curves similar to that in Fig. 2. It is calculated for the same models of proton and neutron pairing (p and nt, Fig. 1) but adopting the APR I EOS. The curves show the cooling of neutron stars with masses from 1.01 to $M_{\max} = 1.92\,M_\odot$. The density of cooling curves reflects the probability to detect such stars provided the mass distribution of stars is flat in the indicated mass range (and observational selection effects are absent). Stars with $M \leqslant M_{\rm D} = 1.83\,M_\odot$ would have temperatures nearly in the same range as in Fig. 2 (see Section 3). By opening the direct Urca we get a new but rare population of very cold neutron stars ($M_{\rm D} \leqslant M \leqslant M_{\max}$). Taking into account the difficulties to detect such stars, the chances to observe them are really low. Notice that if the EOS would allow higher $M_{\max}$ we could obtain a new dense bunch of curves for very cold stars with $M \approx M_{\max}$.

The same effects are demonstrated in Fig. 5. It shows $T_{\rm s}^\infty$ versus M (left) or $\rho_{\rm c}$ (right) for stars of the Vela pulsar age, $t = 1.66 \times 10^4$ yrs. We present the curves for superfluid stars with the EOSs APR I, II, and III. The horizontal dotted lines give the observational limits of $T_{\rm s}^\infty$ for the Vela pulsar.

One can see a very sharp fall of $T_{\rm s}^\infty$ in the narrow mass range from $M = M_{\rm D}$ to $M = M_{\rm D} + 0.01M_\odot$ for the APR I EOS and especially for APR II. This fall is naturally associated with the strong enhancement of the neutrino luminosity by the direct Urca process.

The case of ARP III is different. As seen in Fig. 1, the threshold of opening the direct Urca process is placed now in a wide region near the maximum of the critical temperature $T_{\rm cnt}(\rho)$. When the internal stellar temperature falls noticeably below $T_{\rm cnt}(\rho)$ in some region of $\rho > \rho_{\rm D}$, the suppression of the direct Urca process by neutron superfluidity becomes important and smears out the dependence of $T_{\rm s}^\infty$ on M. The similar effect of partial suppression of the direct Urca process by superfluidity was discussed by Page & Applegate (1992).

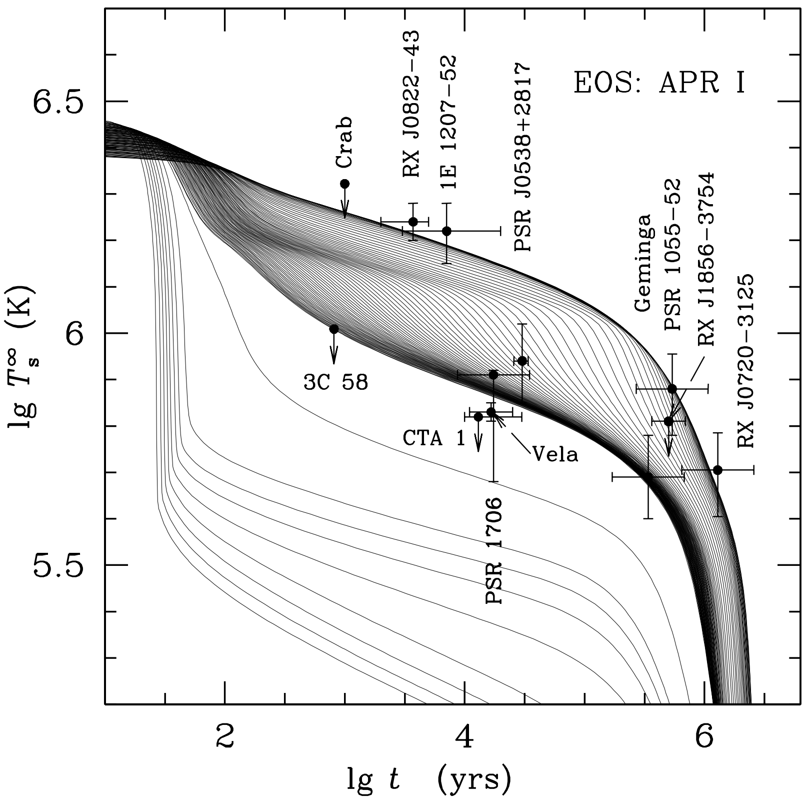

Figure 4. Same as in Fig. 2 but for the EOS APR I. Ninety two cooling curves refer to neutron stars of masses from 1.01 to $M_{\max} = 1.92\ M_\odot$ (with the step $0.01 M_\odot$). The sharp boundary between densely and rarely covered domains corresponds to the direct Urca threshold, $M_D = 1.83 M_\odot$ (Table 2).

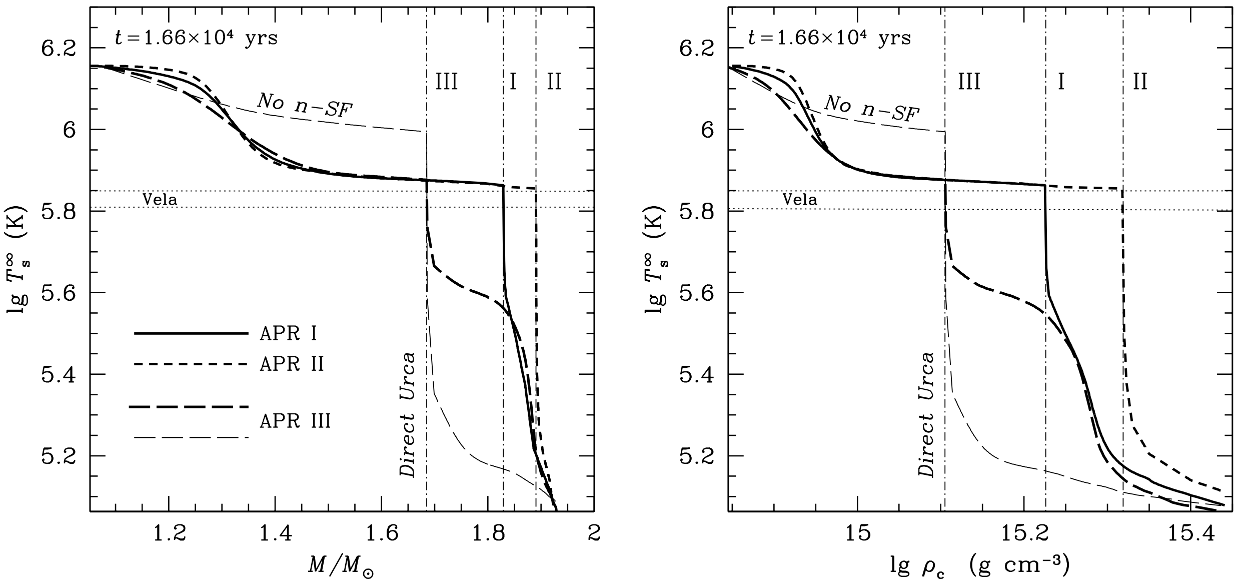

Figure 5. Surface temperatures of neutron stars of the age of Vela pulsar, $t = 1.66 \times 10^4$ yr, versus stellar mass (left) and central density (right) for three EOSs (Table 2): APR I (solid lines), APR II (short dashes), and APR III (thin and thick long dashes), assuming either combined proton and neutron (p and nt) pairing in stellar cores (thick lines) or only proton pairing alone (*No* n-*SF*; thin lines). The vertical dot-and-dashed lines, denoted by I, II, and III, show the threshold masses M_D (left) or densities ρ_D (right) for the direct Urca process. Horizontal dotted lines are observational limits on the Vela's surface temperature.

Evidently, the level of this suppression is regulated by the strength and density range of neutron pairing and by the threshold density of the direct Urca process. Were neutron superfluidity absent (the thin long-dashed line), the dependence would be as sharp as for the EOSs ARP I and II.

The dependence of T_s^∞ on ρ_c (the right panel of Fig. 5) is similar to the dependence on M. Note only much smoother dependence of T_s^∞ on ρ_c in the lower parts of the curves; small variations of $M \lesssim M_\mathrm{max}$ correspond to larger variations of ρ_c (Fig. 3).

Figure 6 is similar to Figs. 2 and 4 and shows cooling curves calculated for the APR III EOS and the same models for proton and neutron pairing (p and nt). Neutron star masses range from 1.01 to $M_\mathrm{max} = 1.93\ M_\odot$. A sharp lower boundary of the densely covered domain corresponds to the direct Urca threshold $M_\mathrm{D} = 1.68 M_\odot$. In contrast to Fig. 4, we now obtain a representative (densely populated) family of middle-aged neutron stars with $M > M_\mathrm{D}$ and $\lg T_\mathrm{s}^\infty \approx 5.6-5.7$. They are much colder than stars with $M < M_\mathrm{D}$ but much hotter than those with $M \approx M_\mathrm{max}$. They appear owing to the flattening of the dependence T_s^∞ on M by neutron superfluidity (Fig. 5). Were this cooling scenario realized in the nature, the chances to detect such stars would be higher than for the scenario in Fig. 4.

The comparison of Figs. 4 and 6 shows a slight increase of the gap between the lower boundary $T_\mathrm{s}^\infty(t)$ of densely populated family of neutron stars with $M < M_\mathrm{D}$ and the observed surface temperature of the Vela pulsar. This difference is also illustrated in Fig. 5; the curves $T_\mathrm{s}^\infty(M)$ and $T_\mathrm{s}^\infty(\rho_\mathrm{c})$ merge in nearly the same slowly decreasing function before the direct Urca thresholds ($M < M_\mathrm{D}$, $\rho_\mathrm{c} < \rho_\mathrm{D}$).

5 DISCUSSION AND CONCLUSIONS

We have extended the scenario of neutron star cooling proposed in Papers I and II to the class of EOSs which allow the operation of the powerful direct Urca process in the cores of massive stars. It widens possible interpretations of observational data on thermal emission from isolated middle-aged neutron stars using simplest models of neutron star cores composed of nucleons, electrons, and muons.

The main common feature of our present scenario and the scenarios of Papers I and II is that the enhanced neutrino emission, required for the interpretation of observations of coldest neutron stars, is produced by Cooper pairing of neutrons. This puts stringent constraints (Paper I) on the density dependence of the critical temperature $T_\mathrm{cnt}(\rho)$ for triplet-state neutron pairing. Tuning our phenomenological model of $T_\mathrm{cnt}(\rho)$ we have obtained a noticeable dependence of cooling on neutron star mass M.

In the scenario of Paper I we have also needed strong proton pairing in the outer cores of neutron stars to explain the observations of neutron stars hottest for their age. In Paper II we have extended that scenario taking into account a possible presence of accreted envelopes and singlet-state pairing of neutrons in the stellar crust. We have shown that the presence of accreted envelopes allows us to take weaker proton pairing. Note, that models of weaker pairing are consistent with recent microscopic calculations of proton critical temperatures (Zuo et al. 2004, Takatsuka & Tamagaki 2004), although some other calculations predict much stronger proton pairing (e.g., Lombardo & Schulze 2001; also see references in Yakovlev et al. 1999, and a recent paper by Tanigawa et al. 2004).

In this paper, for simplicity, we use the model of strong proton pairing in the stellar core. However, following Paper II, we could assume the presence of accreted envelopes, which would again allow us to weaken proton pairing. Adopting moderately strong proton pairing (with $T_\mathrm{cp}^\mathrm{max} \gtrsim 10^9$ K) we could interpret the observations of neutron stars warmest for their age.

The main feature of this paper is the consideration of EOSs which open the direct Urca process in central layers ($\rho \gtrsim 10^{15}$ g cm^{-3}) of most massive stars. We have employed the parameterization of the EOS of Akmal et al. (1998) proposed by Heiselberg & Hjorth-Jensen (1999, 2000). In combination with properly chosen phenomenological models for strong proton pairing ($T_\mathrm{cp}^\mathrm{max} \gtrsim 5 \times 10^9$ K at $\rho \lesssim 8 \times 10^{14}$ g cm^{-3}) and moderate neutron pairing ($T_\mathrm{cnt}^\mathrm{max} \sim 6 \times 10^8$ K at $\rho \gtrsim 10^{15}$ g cm^{-3}) it allows us to predict new types of cooling neutron stars, in addition to those given by the cooling scenario without any direct Urca process (Papers I and II, Sect. 3). They are rapidly cooling neutron stars with masses higher than the direct Urca threshold mass M_D. We have shown (Section 4) that the family of these stars can be either rarely populated (Fig. 4) and thus difficult to discover, or rather distinct and populated (Fig. 6), depending on the choice of a model EOS of dense matter and a model for neutron superfluidity. Neutron stars from the distinct class could be cold but much warmer than massive stars with the fully open direct Urca process.

There is no clear evidence for the existence of such cold stars at the moment but it may appear in the future. For instance, low upper limits on thermal emission from hypothetical neutron stars in a few supernova remnants (Kaplan et al. 2004) can be treated as an indirect indication of the existence of such cold stars. In this context the new scenario would allow one to explain the existence of these cold objects (if discovered) in the frame of standard and simple physics of dense matter (without assuming the presence of hyperons and/or exotic forms of matter, such as pion/kaon condensates or quarks).

As has already been emphasized, we need neutron pairing to explain the current observations of stars coldest for their age. However, according to Gusakov et al. (2004b), cooling curves are not too sensitive to exchanging $T_\mathrm{cp}(\rho) \rightleftharpoons T_\mathrm{cnt}(\rho)$ in neutron star cores. Therefore, we would also be able to explain the data assuming strong neutron pairing and moderate proton pairing in stellar cores.

Finally, let us note that the same physics of neutron star interiors, which is tested by observations of isolated (cooling) neutron stars, can also be tested by observations of accreting neutron stars in soft X-ray transients (e.g., Yakovlev, Levenfish & Haensel 2003) basing on the hypothesis of deep crustal heating of such stars (Brown, Bildsten, Rutledge 1988) by pycnonuclear reactions in accreted matter (Haensel & Zdunik 1990). The observations of soft X-ray transients in quiescent states indicate (Yakovlev, Levenfish & Gnedin 2005) the existence of rather cold neutron stars (first of all, SAX J1808.4–3658) inconsistent with the minimal model of cooling neutron stars. Although these observations are currently inconclusive (e.g., Yakovlev et al. 2005), if confirmed in future observations,

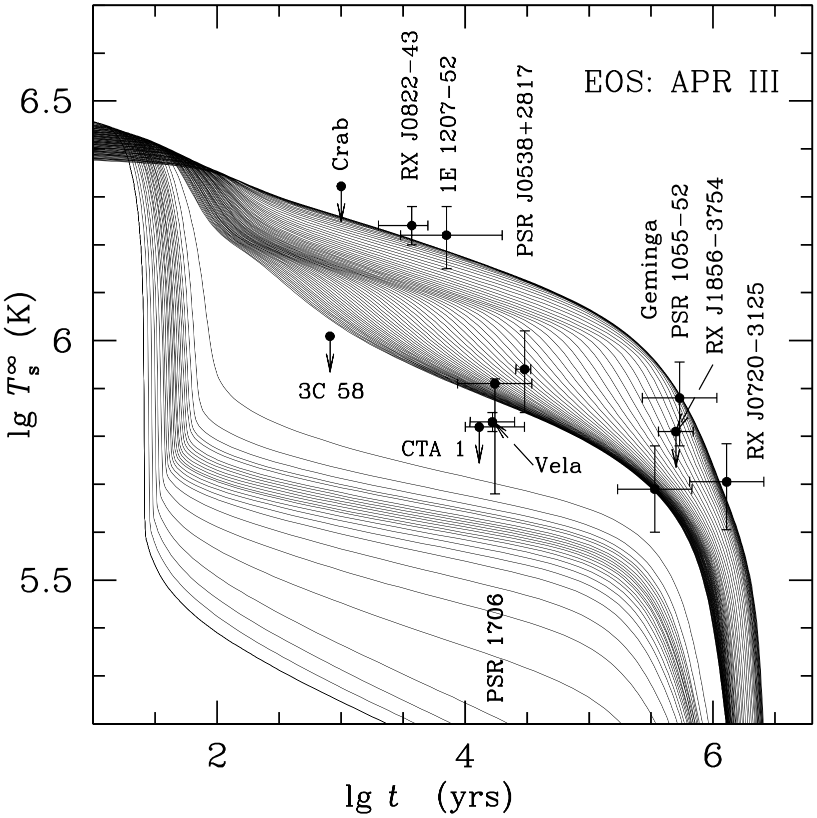

Figure 6. Same as in Figs. 2 and 3 but for the APR III EOS. Ninety three thin solid curves refer to neutron stars of masses from 1.01 to $M_{\max} = 1.93\,M_\odot$ (with the step $0.01\,M_\odot$). The lower boundary of the densely covered domain refers to the direct Urca threshold, $M_{\rm D} = 1.68 M_\odot$.

they could give an evidence in favor of the cooling scenario proposed in this paper.

Acknowledgments We are grateful to A.Y. Potekhin for providing us with fit parameters for the APR EOS, as well as to A.M. Krassilchtchikov and K.P. Levenfish for assistance in drawing figures. We are also grateful to anonymous referee for critical remarks. This work has been supported partly by the RFBR (grants 05-02-16245 and 03-07-90200), the program Russian Leading Scientific School (grant 1115.2003.2), the Russian Science Support Foundation, and by the INTAS (grant YSF 03-55-2397).

References

Akmal A., Pandharipande V. R., Ravenhall D. G., 1998, Phys. Rev. C, 58, 1804
Brown E.F., Bildsten L., Rutledge R.E., 1998, ApJ, 504, L95
Douchin F., Haensel P., 2001, A&A, 380, 151
Flowers E. G., Ruderman M., Sutherland P. G., 1976, ApJ, 205, 541
Gnedin O. Y., Yakovlev D. G., Potekhin A. Y., 2001, MNRAS, 324, 725
Gusakov M. E., Kaminker A. D., Yakovlev D. G., Gnedin O. Y., 2004a, A&A, 423, 1063 (Paper I)
Gusakov M. E., Kaminker A. D., Yakovlev D. G., Gnedin O. Y., 2004b, Astron. Lett., 30, 759
Haensel P., Potekhin A.Y., 2004, A&A, 428, 191
Haensel P., Zdunik J.L., 1990, A&A, 227, 431
Halpern J. P., Gotthelf E. V., Camilo F., Helfand D.J., Ransom S. M., 2004, ApJ, 612, 398
Heiselberg H., Hjorth-Jensen M., 1999, ApJ, 525, L45
Heiselberg H., Hjorth-Jensen M., 2000, Phys. Rep., 328, 237
Kaminker A. D., Yakovlev D. G., Gnedin O. Y., 2002, A&A, 383, 1076
Kaminker A. D., Gusakov M. E., Yakovlev D. G., Gnedin O. Y., 2005, MNRAS, submitted (Paper II)
Kargaltsev O.Y., Pavlov G.G., Zavlin V.E., Romani R.W., 2005, ApJ, in press [astro-ph/0502076]
Kaplan D. L., Frail D. A., Gaensler B. M., Gotthelf E. V., Kulkarni S. R., Slane P. O., Nechita A., 2004, ApJSS, 153, 269
Lattimer J. M., Pethick C. J., Prakash M., Haensel P., 1991, Phys. Rev. Lett., 66, 2701
Lombardo U., Schulze H.-J., 2001, in Blaschke D., Glendenning N. K., Sedrakian A., eds, Physics of Neutron Star Interiors, Springer, Berlin, p. 30
McGowan K. E., Zane S., Cropper M., Kennea J. A., Córdova F. A., Ho C., Sasseen T., Vestrand W. T., 2004, ApJ, 600, 343
Motch C., Zavlin V. E., Haberl F., 2003, A&A, 408, 323

Page D., Applegate J. H., 1992, ApJ, 394, L17

Page D., Lattimer J. M., Prakash M., Steiner A. W., 2004, ApJS, 155, 623

Pavlov G. G, Zavlin V. E, Sanwal D., 2002, in: Becker W., Lesh H., Trümper J., eds, 270 WE-Heraeus Seminar on Neutron Stars, Pulsars and Supernova Remnants, MPE: Garching, p. 273

Pavlov G. G, Zavlin V. E., 2003, in Bandiera R. , Maiolino R., Mannucci F., eds, XXI Texas Symposium on Relativistic Astrophysics, Singapore, World Scientific Publishing, p. 319

Potekhin A. Y., Yakovlev D. G., Chabrier G., Gnedin, O. Y., 2003, ApJ, 594, 404

Schwenk A., Friman B., 2004, Phys. Rev. Lett., 92, 082501

Slane P., Helfand D. J., Van der Swaluw E., Murray S. S., 2004, ApJ, 616, 403

Takatsuka T., Tamagaki R., 1997, Prog. Theor. Phys., 97, 345

Takatsuka T., Tamagaki R., 2004, Nucl. Phys., A738, 387

Tanigawa T., Matsuzaki M., Chiba S., 2004, Phys. Rev., C70, 065801

Weisskopf M. C., O'Dell S. L., Paerels F., Elsner R. F., Becker W., Tennant A. F., Swartz D. A., 2004, ApJ, 601, 1050

Yakovlev D. G., Pethick C. J., 2004, Ann. Rev. Astron. Astrophys., 42, 169

Yakovlev D. G., Levenfish K. P., Shibanov Yu. A., 1999, Physics – Uspekhi, 42, 737

Yakovlev D.G., Levenfish K.P., Haensel P., 2003, A&A, 407, 265

Yakovlev D.G., Levenfish K.P., Gnedin O.Y., 2005, Europ. Phys. J., A, in press [astro-ph/0501653]

Zavlin V. E., Pavlov G. G., 2004, in Proc. XMM-Newton EPIC Consortium Memorie della Societa' Astronomica Italiana, 75, 458

Zavlin V. E., Trümper J., Pavlov G. G., 1999, ApJ, 525, 959

Zavlin V. E., Pavlov G. G., Sanwal D., 2004, ApJ, 606, 444

Zuo W., Li Z. H., Lu G. C., Li J. Q., Scheid W., Lombardo U., Schulze H.-J., Shen C. W., 2004, Phys. Lett., B595, 44